Available online at www.sciencedirect.com
SCIENCE DIRECT®
Physica B 334 (2003) 408–412
PHYSICA B
www.elsevier.com/locate/physb

Grain boundary effects on the magneto-transport properties of Sr_2FeMoO_6 induced by variation of the ambient H_2–Ar mixture ratio during annealing

C.L. Yuan[a], Y. Zhu[a], P.P. Ong[a,*], C.K. Ong[b], T. Yu[a], Z.X. Shen[a]

[a] *Department of Physics, National University of Singapore, 2 Science Drive 3, Singapore 117542, Singapore*
[b] *Department of Physics, Centre for Superconducting and Magnetic Materials, National University of Singapore, 2 Science Drive 3, Singapore 117542, Singapore*

Received 28 March 2003; received in revised form 28 March 2003; accepted 29 March 2003

Abstract

Using the sol–gel method, polycrystalline double perovskites Sr_2FeMoO_6 with nanometer-scale grain size have been synthesized in the ambience of a controlled stream of different gaseous H_2–Ar mixtures during annealing. X-ray diffraction (XRD) results indicated that with an increasing proportion of H_2, the component of the $SrMoO_4$ impurity present in the crystallites first decreased, but then increased again with further increase of the H_2 proportion. The XRD results were further supported by independent sample analysis using Raman spectroscopy. Systematic investigation of the transport properties of the samples indicated that the $SrMoO_4$ impurity at the grain boundary played a key role in determining the measured resistance and magnetoresistance of Sr_2FeMoO_6. This impurity effect was found to be correlated to the variation of the mixture ratio of the ambient H_2–Ar gas stream surrounding the sample during annealing.

PACS: 72.15.Gd; 73.40.Gk; 75.50.Cc

Keywords: Magnetoresistance; Grain boundaries; Double perovskites

Recently, double perovskite Sr_2FeMoO_6 was established as a new colossal magnetoresistive (CMR) material [1]. This compound has one of the highest critical temperatures ($T_c \sim 410$ K) among the half-metals, thus greatly enhancing its possibility for applications. Compared to the perovskite-like manganites, the double perovskites have the advantage of large low-field room-temperature magnetoresistance (MR) which is quite insensitive to temperature changes. The unique character of Sr_2FeMoO_6 is that its transport properties are dominated by spin-polarized tunneling through insulating grain boundaries [2]. The nonmagnetic $SrMoO_4$ impurity was found to be induced to appear at the grain boundaries [3], and the conducting properties of Sr_2FeMoO_6 depend sensitively on the history and annealing time of the precursor. Moreover, the level of the $SrMoO_4$ impurity is intimately correlated to the mixture ratio of the ambient gaseous H_2–Ar

*Corresponding author. Tel.: +65-68748002; fax: +65-67776126.
E-mail address: phyongpp@nus.edu.sg (P.P. Ong).

0921-4526/03/$ - see front matter
doi:10.1016/S0921-4526(03)00124-8

stream passing over the material during its high-temperature sintering. Therefore, we can in principle adjust the MR properties of Sr_2FeMoO_6 by controlling the $SrMoO_4$ impurity through a variation of the mixture ratio of the gaseous H_2–Ar stream.

Raman scattering has been used to investigate CMR materials [4] and the structures of the polycrystalline Sr_2FeMoO_6 [5]. Therefore, in this paper, in addition to the current empirical work, a micro-Raman-scattering method was also employed to investigate the variation of the content of $SrMoO_4$ impurity in the polycrystalline Sr_2FeMoO_6.

Bulk Sr_2FeMoO_6 samples were prepared by the sol–gel method, followed by heat treatment at different temperatures [6]. Briefly, the method consisted of weighing stoichiometric quantities of $(NH_4)_6Mo_7O_{24}\cdot 4H_2O$, $Fe(NO_3)_3\cdot 9H_2O$, and $Sr(NO_3)_2$, preparing them in solution form, and mixing the solutions of $Sr(NO_3)_2$, and $(NH_4)_6Mo_7O_{24}\cdot 4H_2O$ with nitric acid according to the proportion of $\sim$10 times moles of $(NH_4)_6Mo_7O_{24}\cdot 4H_2O$. The resultant mixture was then mixed with a solution of $Fe(NO_3)_3\cdot 9H_2O$ to form a light green gel after several minutes. The gel was dried at 60°C. Subsequently, the powder was obtained by high-energy ball milling for 3 h. It was then preheated at 700°C for 6 h and further milled by high-energy ball milling for another 3 h. Finally, the powder was pressed into pellets followed by sintering at 900°C in the ambience of a controlled stream of various proportions of gaseous H_2–Ar mixtures for 3 h. The resulting test samples obtained by sintering in a stream of 3%, 5% and 7% of H_2 to Ar in the gas mixture are labeled A, B and C, respectively.

The crystal structure and phase purity of the samples were examined by X-ray diffraction using Cu K_α radiation. All micro-Raman spectra were measured in the backscattering geometry using an ISA Jobin–Yvon–Spex T64000 Raman spectrometer with an Olympus microscope attachment. The 514.5 nm line of an argon-ion laser was used as the excitation source. The electrical resistivity ρ was measured using the standard four-probe technique in the temperature range from 78 to 300 K. The magnetoresistivity ratio, MR, is defined as $MR\,(\%) = \Delta\rho/\rho_0 \times 100\%$ where $\Delta\rho = \rho_0 - \rho_H$, and ρ_H and ρ_0 are, respectively, the resistivities in an applied magnetic field and in zero field.

X-ray diffraction patterns of the three samples are shown in Fig. 1. The inset shows the expanded section in the range $25° < 2\theta < 30°$ containing the strongest peak originating from the $SrMoO_4$ impurity. All the XRD peaks of sample B and the peaks of the main phase of Sr_2FeMoO_6 except for the peaks of $SrMoO_4$ of samples A and C can be indexed according to the space group I4/mmm. With increasing proportion of H_2, the $SrMoO_4$ impurity content first decreased, and then increased again. It was estimated that the relative contents of $SrMoO_4$ in the samples A, B and C were about 2.9%, 0.4% and 3.5%, respectively. Further analysis of the X-ray powder diffraction

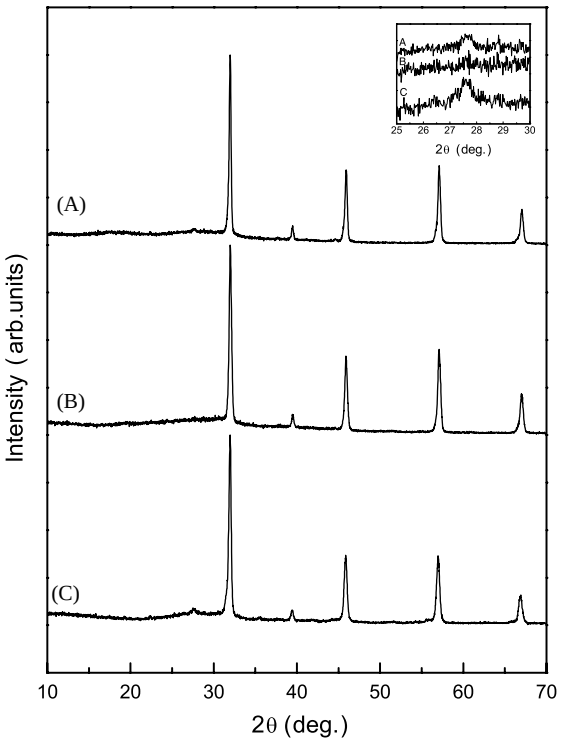

Fig. 1. X-ray diffraction patterns of polycrystalline Sr_2FeMoO_6 samples prepared under different H_2–Ar mixture ambience. Sample A: 3% H_2, B: 5% H_2, and C: 7% of H_2 to Ar in the gas mixture. The magnified section in the range $25° < 2\theta < 30°$ containing the strongest peak of the $SrMoO_4$ impurity phase is shown in the inset.

pattern in terms of the Rietveld analysis indicated that the degrees of cation ordering in the samples A, B and C were about 97%, 99% and 96%, respectively.

Fig. 2 shows the Raman spectra of the three samples at room temperature. The peak at 882.3 cm^{-1}, labeled "*", corresponds to the strongest line in the Raman-scattering spectra of the $SrMoO_4$ impurity phase. It is obvious from the curves that the amounts of the $SrMoO_4$ impurity in samples A and C were each much more than that of sample B. Thus, this result reinforces the conclusion obtained in the XRD analysis in Fig. 1.

Fig. 3 shows the temperature dependence of the resistivities at zero field and at 1 T, respectively, for the three samples. Samples A and C show semiconductor behavior with their resistivities decreasing with temperature over the entire measured temperature range. In contrast, sample B shows metallic behavior over almost the same temperature range. The resistivities of sample B are also smaller than those of samples A and C. These surprising results are found to be correlated to the different $SrMoO_4$ impurity contents. Because the nonmagnetic $SrMoO_4$ impurity is induced to appear at the grain boundaries, and the transport property of the sample is determined by electron tunneling between grains, the higher resistivity and semiconductor behavior of samples A and C, and the metal behavior of sample B, can all be ascribed to the prevailing contribution of the grain boundary, which is known to form tunneling barriers for carrier transport. Clearly, the enhanced $SrMoO_4$ impurity level in samples A and C also enhances the grain boundary effect on their resistivities.

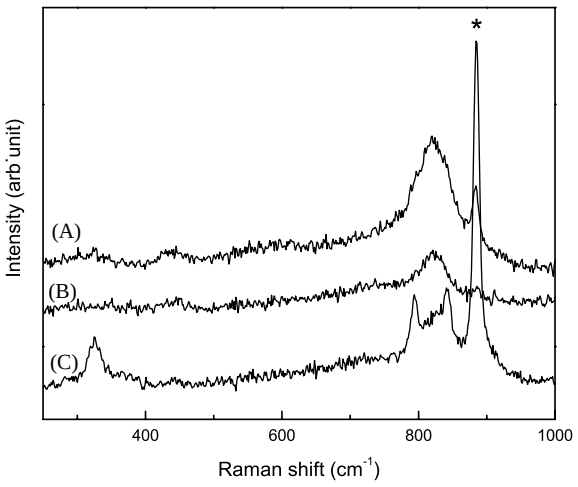

Fig. 2. Raman spectra of samples A, B and C prepared under different H_2–Ar mixture ambience at room temperature. The peak pertaining to the impurity $SrMoO_4$ is indicated by "*".

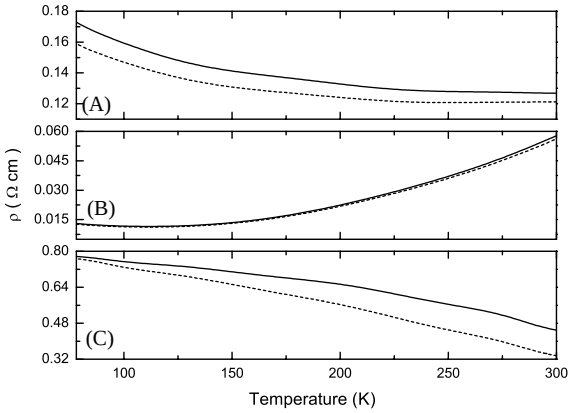

Fig. 3. Temperature dependence of resistivity for Sr_2FeMoO_6 samples prepared under different H_2–Ar mixture ambience at zero field (—) and at 1 T (- - -).

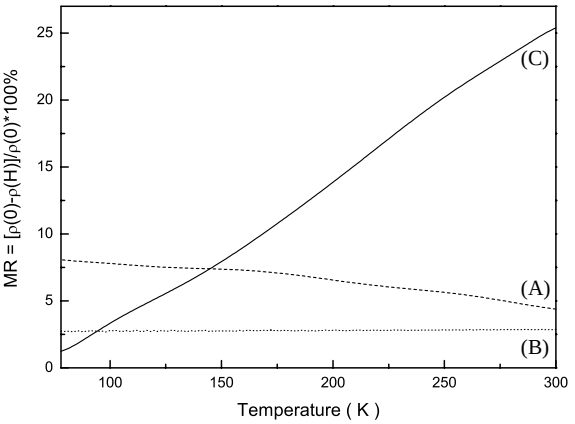

Fig. 4. Temperature dependence of the magnetoresistivity ratio $MR(\%) = (\rho_0 - \rho_H)/\rho_0 \times 100\%$ for Sr_2FeMoO_6 at $H = 1$ T. Sample A: dashed line; B: dotted line; C: continuous line.

The temperature dependence of the magnetoresistivity ratio $MR(\%) = \Delta\rho/\rho_0 \times 100\%$ ($\Delta\rho = \rho_0 - \rho_H$) at 1 T for the three samples is shown in Fig. 4. Resistivity measurements in a magnetic field of 1 T showed only a small MR effect for the

metallic sample B, but a significantly larger magnetoresistive response for the semiconducting samples A and C. This result clearly demonstrates that for samples A and C, the enhancement of the IMR is correlated with the large effective intergrain-tunneling barrier arising from the increased level of the impurity $SrMoO_4$. It is well known that the low-field MR increases as the temperature decreases due to the rise in spin polarization. However, the measurements for sample C show that the MR decreases as the temperature decreases and also its unusually high value at room temperature. This phenomenon appears to be attributable to the competition between the coexistent metallic Sr_2FeMoO_6 phase and the insulating $SrMoO_4$ impurity phase. Similar competition between the coexistent metallic phase and the insulating phase was also found in (La, Pr, Ca)MnO_3 [7], $La_{1-x}Sr_xCoO_3$ [8] and $Sr_2Fe_{1-x}Cu_xMoO_6$ [9], which depressed the metal–insulator transition temperature [10]. For sample C, the competition between the coexistent metallic Sr_2FeMoO_6 phase and the insulating $SrMoO_4$ impurity phase could also be responsible for the decrease of the metal–insulator transition temperature at high temperatures, thus enhancing the low-field MR near the metal–insulator transition temperature. Further investigation on the magnetoresistive behavior at high temperatures is being made at present.

The mixture ratio of the stream of gaseous H_2–Ar mixture strongly affects the eventual nonmagnetic $SrMoO_4$ impurity level in the annealed material, thereby determining whether its resistivity would exhibit metallic or semiconducting behavior. This $SrMoO_4$ impurity level, in turn, plays a crucial role in determining the low-magnetic-field intergrain tunneling MR. The presence of the impurity leads to an enhancement of the intergrain tunneling barrier, with a consequential increase in the resistivity and the low-field MR. The magnetic domain reorientation in the polycrystalline Sr_2FeMoO_6 can be controlled by the application of a magnetic field, which tends to parallelize the magnetization directions of the ferromagnetic domains. The corresponding reduction in the spin scattering of spin-polarized carriers at the grain boundaries gives rise to a significant decrease of the measured resistivity [1]. When the intergrain barrier diminishes, the itinerant electrons in the surface of each grain become delocalized between the two neighboring grains. This delocalization would be brought about by a reduction in the misalignment between the localized t_{2g} spins located at the surface of the two grains, thus reducing the effective angle θ between the magnetizations of neighboring grains at zero field. The intergrain barrier is diminished, resulting in a suppression of the low-field MR [3,11].

If a large magnetoresistivity ratio at high temperatures is required, one may consider increasing the imperfections at the grain boundaries. For example, it will be quite easy to enhance the magnetoresistivity by raising the intergrain barrier layer with a corresponding increase in the $SrMoO_4$ impurity at the grain boundaries, which can in turn be controlled by adjusting the mixture ratio of the ambient H_2–Ar stream surrounding the sample during its high-temperature sintering.

In summary, we conclude that the magnetic and electric properties of the Sr_2FeMoO_6 double-perovskite material, its $SrMoO_4$ impurity level, and the environmental ambience of different H_2–Ar mixtures in the annealing treatment of the material are all inter-related, thereby providing us a simple means to control the transport properties by tuning the ambient gaseous mixture ratio.

Acknowledgements

This work was supported under NUS Research Grant No. R-144-000-011-012 and R-144-000-064-112.

References

[1] K.-I. Kobayashi, T. Kimura, H. Sawada, K. Terakura, Y. Tokura, Nature (London) 395 (1998) 667.
[2] T.H. Kim, M. Uehara, S.-W. Cheong, S. Lee, Appl. Phys. Lett. 74 (1999) 1737.
[3] D. Niebieskikwiat, A. Caneiro, R.D. Sánchez, J. Fontcuberta, Phys. Rev. B 64 (2001) 180406.

[4] V. Dediu, C. Ferdeghini, F.C. Matacotta, P. Nozar, G. Ruani, Phys. Rev. Lett. 84 (2000) 4489.
[5] L. Hoang Son, Nguyen Xuan Phuc, Phan Vinh Phuc, Nguyen Minh Hong, Le Van Hong, J. Raman Spectrosc. 10 (2001) 817.
[6] C.L. Yuan, S.G. Wang, W.H. Song, T. Yu, J.M. Dai, S.L. Ye, Y.P. Sun, Appl. Phys. Lett. 75 (1999) 3853.
[7] M. Uehara, S. Mori, C.H. Chen, S.-W. Cheong, Nature (London) 399 (1999) 560.
[8] R. Caciuffoet, R. Caciuffo, D. Rinaldi, G. Barucca, J. Mira, J. Rivas, M.A. Señarís-Rodríguez, P.G. Radaelli, D. Fiorani, Phys. Rev. B. 59 (1999) 1068.
[9] C.L. Yuan, Y. Zhu, P.P. Ong, J. Appl. Phys. 91 (2002) 4421.
[10] D. Niebieskikwiat, R.D. Sánchez, A. Caneiro, L. Morales, M. Vásquez-Mansilla, F. Rivadulla, L.E. Hueso, Phys. Rev. B. 62 (2000) 3340.
[11] H.Y. Hwang, S.-W. Cheong, N.P. Ong, B. Batlogg, Phys. Rev. Lett. 77 (1996) 2041.